1967

Optimum fin spacing for heat transfer per unit length of heat exchange section

Glenn Ellis Miller

Department:

OPTIMUM FIN SPACING FOR HEAT TRANSFER PER UNIT LENGTH OF HEAT EXCHANGE SECTION

BY

GLENN ELLIS MILLER - 1944

A

THESIS

submitted to the faculty of the

UNIVERSITY OF MISSOURI AT ROLLA

in partial fulfillment of the requirements for the

Degree of

MASTER OF SCIENCE IN MECHANICAL ENGINEERING

Rolla, Missouri

1967

Approved by

A. H. Culp, Jr. (advisor) W. J. Sauer

Robert D. Way R. H. Howell

ABSTRACT

This thesis presents the results of an experimental study of the heat-transfer ability of a finned surface as a function of the spacing between fins. The results are expressed as heat transfer per unit length of finned section rather than the heat transfer per fin.

Circumferential steel fins, seven and three-quarter inches in diameter, were used for the investigation. Data was taken for fin spacings ranging from zero to one and one-half inches. The experimental heat-transfer rate to atmospheric air was determined by measuring the volume of saturated steam which condensed in the test section over a measured time interval. Temperature readings were also taken on the outer radius of the fin surface using a radiation pyrometer.

An analytical study of the overall heat transfer per unit length of the test section was broken down into four parts. These were heat transfer from 1) the outer edge of the fins, 2) the pipe through the middle of the fins, 3) lateral fin surfaces by radiation, and 4) the lateral fin surfaces by convection. The values for the first three parts were calculated from theoretical equations and the difference between the sum of the first three parts and the total measured heat transfer resulted in an evaluation of the convection heat transfer from the lateral fin surfaces.

The results of the experiment show the optimum fin spacing for this particular test section to be five-sixteenths of an inch.

The shape of the curve showing the heat-transfer rate per unit length of finned section as a function of fin spacing shows that there is a sharp maximum and that the value of fin spacing is very critical in order to obtain the maximum heat transfer from the test section.

ACKNOWLEDGEMENTS

The author sincerely appreciated the assistance and advice generously given by Professor Archie Culp, faculty advisor, throughout the planning, experimentation, and writing of this thesis project.

The consultation of Dr. H. J. Sauer at various points during the preparation of this work was also appreciated.

The assistance given by Mr. L. N. Anderson and Mr. R.D. Smith during construction of the apparatus and the procuring of materials helped tremendously in building the experimental apparatus.

The author was especially grateful to his wife, Joy, for her encouragement and for her help during the final preparation by typing the report.

TABLE OF CONTENTS

LIST OF FIGURES

NOMENCLATURE

A - Heat Transfer Surface Area, ft^2

C_p - Specific Heat at Constant Pressure, $BTU/lb_m - °F$

g - Acceleration of Gravity, ft/sec^2

Gr - Grashof Number, Dimensionless

h_c - Convection Heat-Transfer Coefficient, $BTU/hr\text{-}ft^2 - °F$

h_r - Radiation Heat-Transfer Coefficient, $BTU/hr\text{-}ft^2 - °F$

k - Thermal Conductivity, $BTU/hr\text{-}ft - °F$

L - Length, ft

Nu - Nusselt Number, Dimensionless

P - Pressure, lb_f/ft^2

Pr - Prandtl Number, Dimensionless

q - Heat-Transfer Rate, BTU/hr

Q - Heat, BTU

T - Temperature, °F

u - Velocity in the x-Direction, ft/sec

v - Velocity in the y-Direction, ft/sec

α - Linear Coefficient of Thermal Expansion, $°F^{-1}$

α_t - Thermal Diffusivity, ft^2/hr

β - Volumetric Coefficient of Thermal Expansion, $°F^{-1}$

δ - Boundary Layer Thickness, ft

ε - Emissivity, Dimensionless

μ - Dynamic Viscosity, $lb_f\text{-}sec/ft^2$

ν - Kinematic Viscosity, $lb_f\text{-}sec\text{-}ft/lb_m$

ρ - Density, lb_m/ft^3

σ - Stefan-Boltzmann Constant, $BTU/hr\text{-}ft^2 - °R^4$

I. INTRODUCTION

The dissipation or absorption of heat between fluids and surfaces is a major facet of many engineering design problems. In most applications this transfer of energy must take place as rapidly as possible and in a limited space. Various means of transferring this thermal energy are available, but the use of extended surfaces or fins is the most widely used method when the combined surface conductance from one of the surfaces is low. This experiment was conducted in order to find that fin spacing which would result in the maximum heat transfer per unit length of heat exchange section for free-convection heat transfer to atmospheric air. Experimental data was taken for various spacings of circular fins with a rectangular profile.

The theory of free-convection heat transfer from a flat, vertical surface may be used to evaluate the convection heat-transfer rate as long as the spacing between adjacent fins is great enough so that no overlapping of the thermal boundary layers results. However, these theoretical equations usually assume a uniform surface temperature which will not occur on extended surfaces. This effect can be compensated for by determining the average temperature on the fin surface for use with these equations. Then the experimental heat-transfer rate for 'wide' spacings can be verified by the theoretical calculations, as will be shown later.

As the fins were placed closer together, in an attempt to obtain a higher heat-transfer rate per unit length of tube, the thermal

boundary layers began to overlap, causing the convection heat-transfer rate per fin to be reduced. Before the optimum fin spacing was reached, the reduction in the convection heat-transfer rate caused by the increased overlapping of the boundary layers was more than compensated by the increased surface area resulting from putting the fins closer together. Consequently, the heat-transfer rate per unit length increased, although the rate from each single fin decreased. The heat-transfer rate per unit length continued to increase until the optimum fin spacing was reached. For fin spacings less than the optimum fin spacing, the reduction in the convective heat-transfer coefficient was so great that the product of the coefficient and surface area, and consequently the heat-transfer rate, started to decrease as the spacing was further decreased.

The convection heat-transfer rate at the optimum spacing between two vertical, flat plates at uniform temperature has been derived by W. Elenbaas. (3)* By assuming an average temperature on the surface of the fins at the optimum spacing, the experimental heat-transfer rate at the optimum spacing could be calculated using the Elenbaas equation for a uniform surface temperature.

In order to analyze the data from the test apparatus, the radiation heat-transfer rate was also considered. This transfer of heat was calculated by using theoretical shape factors combined with the experimentally measured values of emissivities and surface temperatures.

---

* Underlined numbers in parenthesis indicate references listed in the Bibliography.

The performance of fins is usually described by the "effectiveness" or the "efficiency" of the fins. The effectiveness is defined as "the ratio of the heat conducted through the root of the fin to that which would be transferred from the same root area if the fin were not present and if the root temperature remained the same." The efficiency is defined as "the ratio of the total heat dissipated by the fin to that which would be dissipated if the entire fin surface were at the root temperature." (14)

The data contained in this report has very little meaning when applied to the definitions of fin performance as stated above. Therefore, the data has been presented by defining "the efficiency of the finned section" as "the ratio of the actual heat-transfer rate per unit length to the heat-transfer rate per unit length at the optimum fin spacing."

II. THEORY

In order to supplement the experimental data, an analytical study was made to reduce the overall heat-transfer rate into categories. The theory necessary for the analytical study has been presented in this section.

The contact of any fluid with a surface hotter than the fluid results in the transfer of heat from the surface to the fluid. If this fluid is a liquid, almost all of the heat transfer is a result of convection currents. However, if the fluid is a gas, then heat is removed both by convection and radiation. These two processes are considered separately since they are functions of different factors.

A. Convection Heat Transfer

Convection heat transfer is the process during which heat is transferred from a higher to a lower temperature region, within a gas or liquid, due to motion within the fluid. Natural, or free, convection occurs when the fluid motion comes about solely as a result of the density variation caused by thermal expansion or contraction of the fluid as it comes into contact with a heated or a cooled surface.

When a gas, such as air, comes into contact with a heated, vertical, flat plate, a free-convection boundary layer is formed. The boundary layer consists of moving air. The velocity of the rising air is essentially zero both at the surface of the plate and at the outer edge of the boundary layer. It reaches a maximum at a short

distance from the surface of the plate and then decreases more gradually toward the outer boundary.

The fluid flow is laminar as it forms at the lower edge of the vertical plate and then, as the velocity increases, turbulent eddies are formed and the transition to turbulent flow takes place. The distance above the lower edge of the plate at which the turbulent flow begins is dependent upon the fluid properties and the temperature difference. The boundary layer is shown in Fig. 1.

A differential equation describing the motion of the boundary layer within the laminar-flow region has been obtained by using a momentum analysis along with an energy equation. Both of these equations were derived for an elemental control volume within a laminar portion of the boundary layer. Using this approach, the heat-

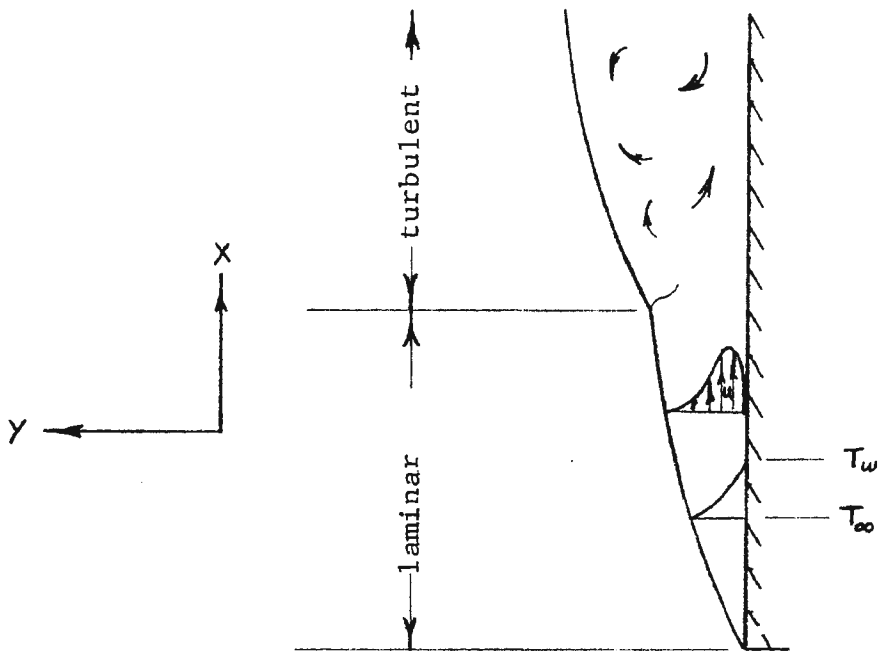

FIG. 1 - CONVECTION BOUNDARY LAYER
ON A VERTICAL, FLAT PLATE

convection coefficient may be expressed in terms of the following dimensionless equation:

$$Nu_x = 0.508\ Pr^{\frac{1}{4}}\ (0.952 + Pr)^{-\frac{1}{4}}\ Gr_x^{\frac{1}{4}}.$$

For much experimental work, the value for the average heat-convection coefficient has been expressed as:

$$\frac{\bar{h}L}{k} = \bar{Nu} = C(GrPr)^m,$$

where the properties are evaluated at the mean film temperatures, defined as:

$$T_f = \frac{T_a + T_w}{2}.$$

The values for C and m have been determined experimentally by McAdams (13) for various ranges of the Grashof-Prandtl number product.

The average heat-convection coefficient may be calculated from the above equation for both vertical, flat plates and horizontal cylinders. A detailed derivation of this equation has been included in the appendix of this report.

W. Elenbaas (4) has made an experimental study of the heat dissipation between two plates, which were placed parallel to each other and at varying distances apart. The experimental test apparatus was constructed such that both plates were heated uniformly over their entire surface areas. Elenbaas applied boundary conditions to the continuity, momemtum, and energy equations which were written for the cooling medium. The temperature and velocity profiles in the spacing between the plates were observed to have shapes as shown in Fig. 2.

By writing mathematical equations for these velocity and tempera-

ture distributions and inserting these expressions into the continuity, momentum, and energy equations, Elenbaas determined a formula for the optimum spacing between the plates and a formula for calculating the average heat-convection coefficient from between the parallel, flat plates. These equations are shown below:

$$b_{opt} = 2.9 \frac{L^{\frac{1}{4}} \mu_s^{\frac{1}{2}} T^{\frac{1}{4}}}{g^{\frac{1}{4}} \rho_s^{\frac{1}{2}} T^{\frac{1}{4}}} ,$$

and $$\bar{h}_c = \frac{k}{b} \bar{Nu} , \quad \text{where} \quad \bar{Nu} = \frac{1}{24} \frac{b}{h} (GrPr) \left[1 - e^{-24 \left(\frac{0.5h}{b(GrPr)} \right)^{3/4}} \right] .$$

The graph on Fig. 3 shows a curve from which the average Nusselt number can be obtained if the Grashof-Prandtl number product is known.

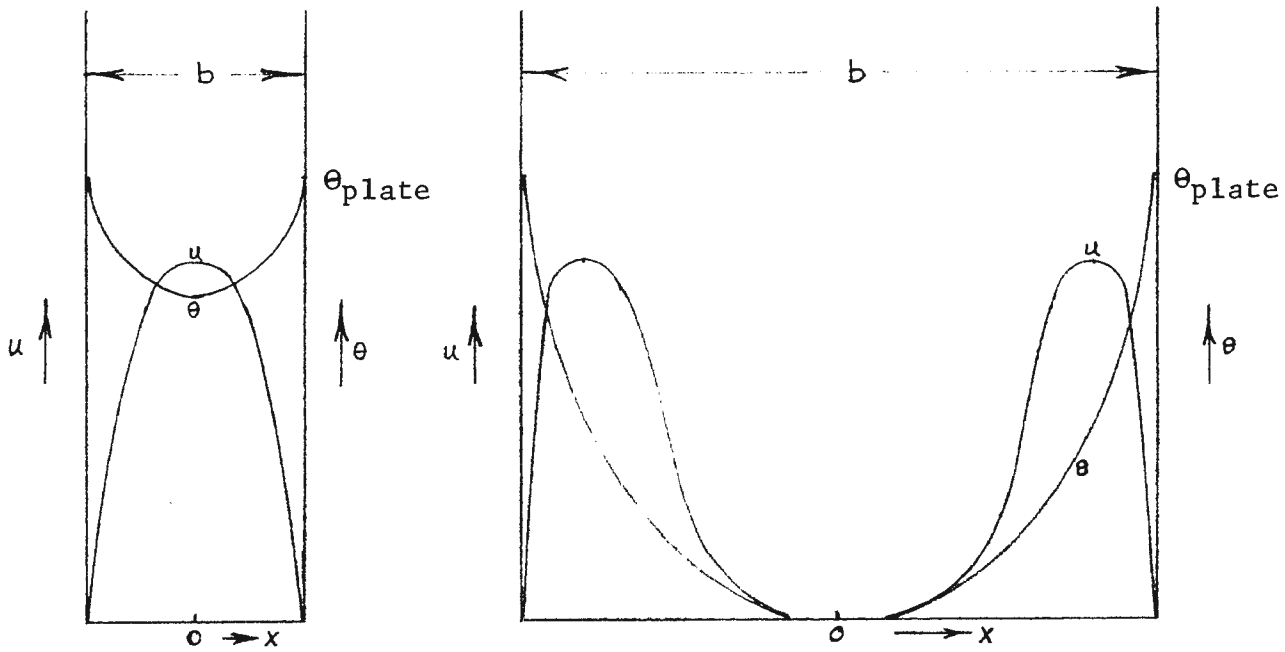

FIG. 2 - TEMPERATURE AND VELOCITY DISTRIBUTIONS BETWEEN PARALLEL, FLAT PLATES OF UNIFORM TEMPERATURE

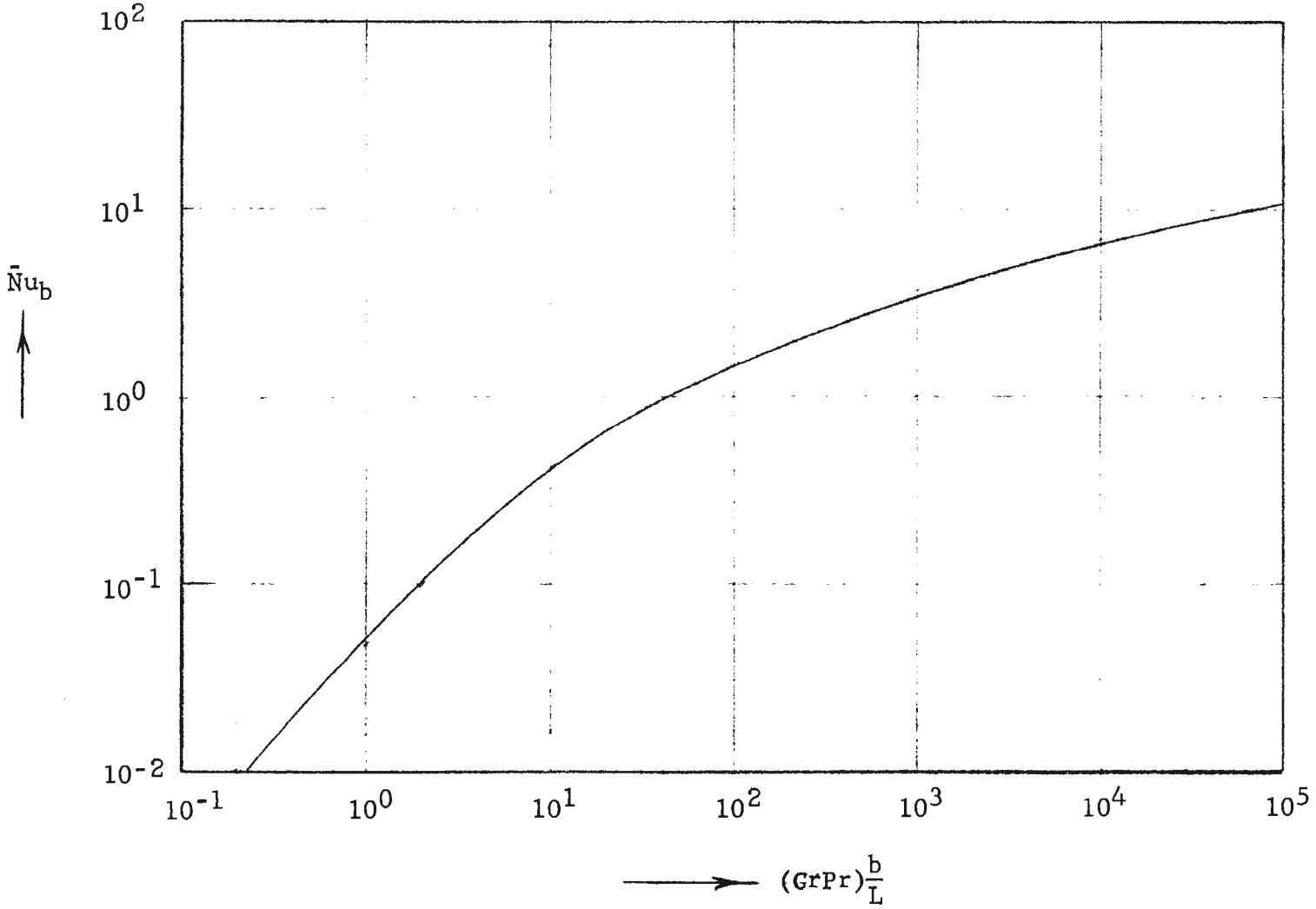

FIG. 3 - RELATIONSHIP BETWEEN THE NUSSELT NUMBER AND THE GRASHOF-PRANDTL NUMBER PRODUCT IN ELENBAAS' EQUATION FOR VARIABLE FIN SPACING

B. Radiation Heat Transfer

Electromagnetic radiation that is exchanged as a result of a temperature difference is known as thermal radiation. Every body will emit thermal radiation proportional to the fourth power of its absolute temperature if the emissivity of the surface is constant. Therefore, the transfer of heat between two surfaces by thermal radiation is proportional to the difference in the fourth power of the absolute temperatures of the adjacent surfaces. The thermal radiation emitted by a surface is also a function of the emissivity of the surface.

Because radiation travels in a straight line, part of this energy will not be transmitted from one fin surface to the adjacent fin surface, but will be radiated into the surroundings. The relationship known as the geometric shape factor may be used to determine the percentage of thermal radiation which is transmitted by one surface and is incident upon an adjacent surface. These shape factors have been determined analytically for many different configurations.

The National Advisory Committee for Aeronautics published Technical Note 2836 in December 1952, giving an analytical formula for determining the shape factor between two concentric, circular disks.

If r_2 = diameter of first disk,

r_1 = diameter of second disk,

d = distance between disks,

$E = r_2/d$,

$D = d/r_1$, and

$x = 1 + (1 + E^2)D^2$,

then the shape factor from the first disk to the second disk is given by (6):

$$F_{1-2} = \tfrac{1}{2}(x - x^2 - 4E^2D^2).$$

This relationship has been used to determine the geometric shape factor for the radiation heat-transfer calculations in this report.

The temperature of a surface may be determined if the thermal radiation which is emitted from that surface can be measured. The propagation of thermal radiation occurs in the form of discrete quanta which may be thought of as having mass, energy, and momentum. Each quantum has an energy of $E = h\nu$, where ν is the frequency and h is Planck's constant. Expressions for the mass and momentum of the particles of radiation have been derived using the relativistic relation between mass and energy, i.e., $E = mc^2 = h\nu$. The energy per unit volume of radiation has been shown to be proportional to the fourth power of the absolute temperature by thermodynamic considerations of the radiation as particles of a gas. This relationship is known as the Stefan-Boltzmann Law. Using this background, the radiation pyrometer was developed to determine the temperature of heated surfaces.

A thermodynamic media, such as water, may exist in the form of a solid, a liquid, or a gas. When water is in the liquid state it will have an energy level which depends upon the temperature and pressure conditions. However, when the liquid reaches its satura-

tion conditions it will remain at the same temperature, provided the pressure remains constant, and will undergo a change of state as it absorbs more energy.

The saturation temperatures for steam are a function of absolute pressure and have been tabulated in Keenan and Keyes book entitled THERMODYNAMIC PROPERTIES OF STEAM. (10) Therefore, if the pressure of saturated steam is known, these tables may be used to determine the temperature and enthalpy. The difference in enthalpy of the saturated steam and the saturated water is the latent heat of vaporization at the pressure under consideration. By measuring the amount of saturated steam which condenses into saturated liquid over a period of time, the heat-transfer rate from the steam container can be determined.

III. DESCRIPTION OF APPARATUS

The test section, as it will be referred to hereafter, consisted of a four-foot length of one-inch diameter aluminum pipe with steel fins spaced along the pipe. The one-quarter-inch-thick, circular steel fins were of rectangular profile and seven and three-quarters inches in diameter. It is shown in Fig. 4, Fig. 5, and Fig. 6.

The aluminum tube was over 99% pure aluminum and the steel fins were constructed of 1020 hot-rolled structural steel. The steel fins were sand blasted in order to obtain a uniform surface finish and emissivity. The surface finish measured approximately 150 rms microinches roughness.

In order to be able to change the spacing between the fins it was necessary to leave sufficient diametrical clearance between the outer diameter of the tube and the inner diameter of the fin so that the fins would slide along the tube at room temperature. However, it was also desirable to make the thermal resistance between the tube and fins as small as possible. In order to accomplish this objective it was necessary to obtain a pressure fit between the tube and fins at the test temperature of 367°F. So the center hole in each fin was machined to within a diametrical clearance of 0.003 inches with the pipe at room temperature. Then, as the test section was heated to experimental temperature, the aluminum and steel both expanded in accordance to their respective coefficients of thermal expansion. The greater expansion of the aluminum, plus the steam pressure inside the pipe, caused a pressure fit between the aluminum tube and the steel fins. The calculations for this fit indicated

FIG. 4 - EXPERIMENTAL TEST APPARATUS

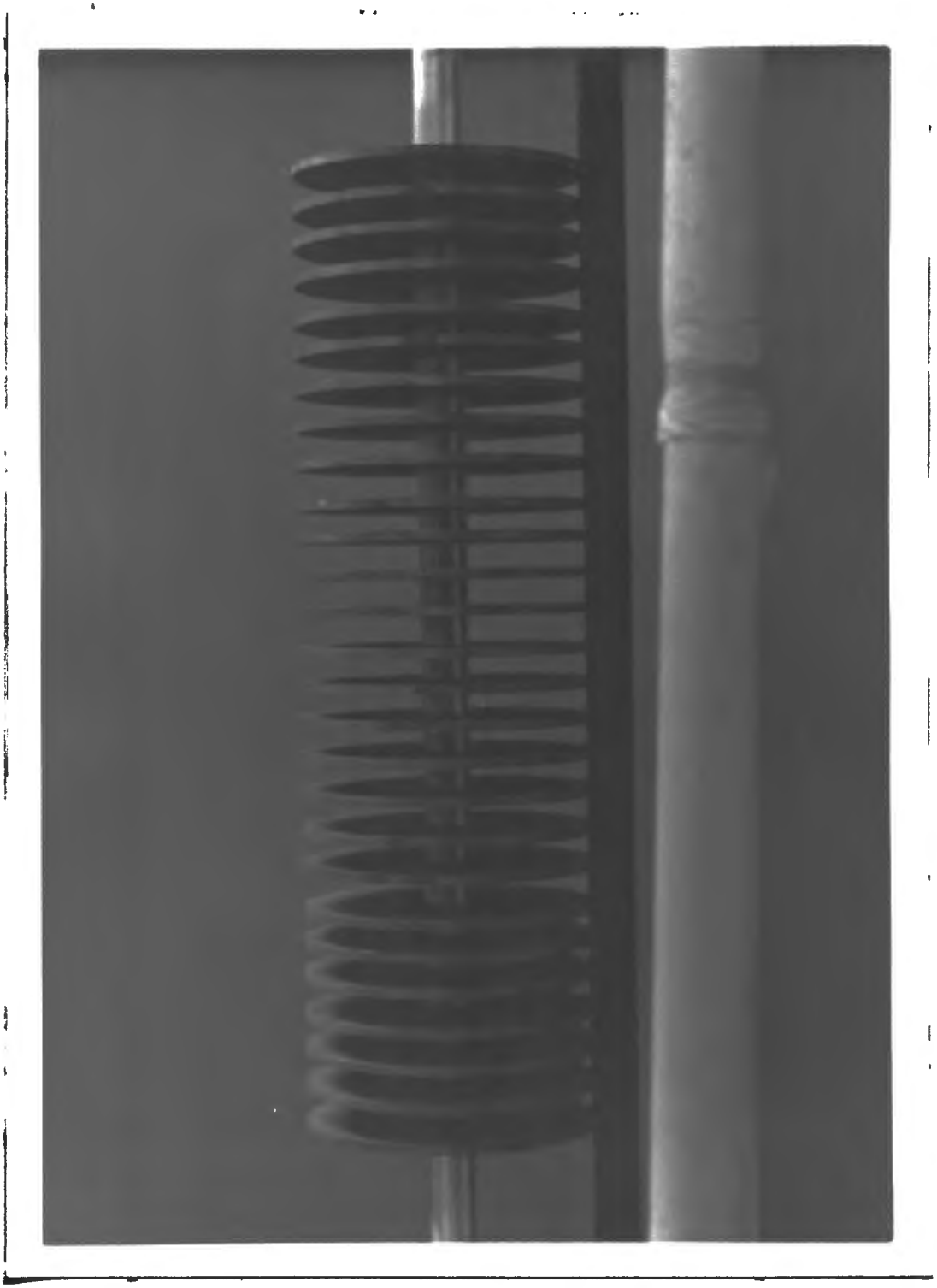

FIG. 5 - FINNED TEST SECTION

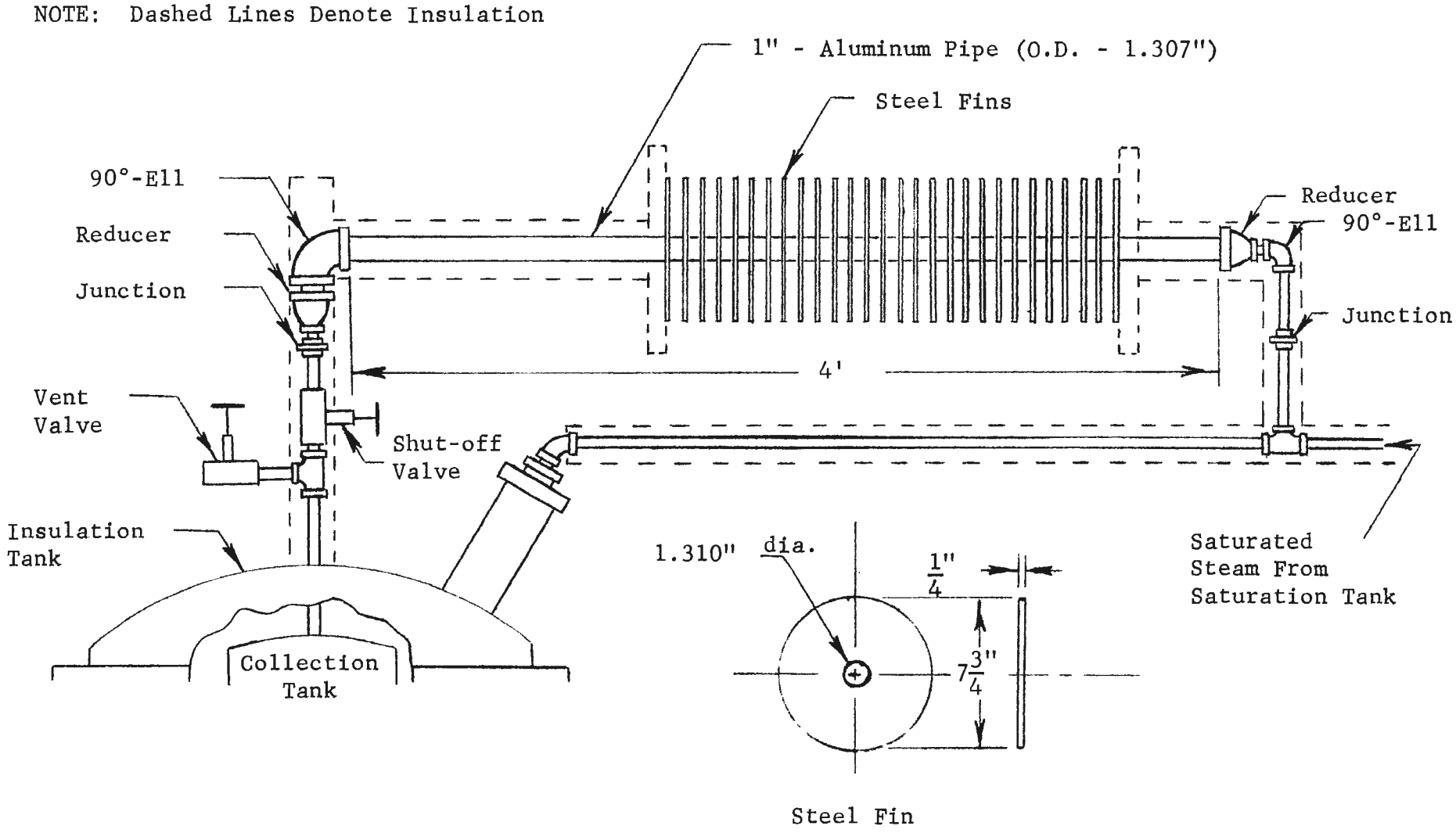

FIG. 6 - TEST SECTION ASSEMBLY

an interference of approximately 0.002 inches to insure a proper pressure fit. In calculating the pressure fit an assumption was made that the fins approximated a sharp-edged ring load on the aluminum tube. (7)

The magnitude of the thermal resistance across an interface with a pressure fit is negligible when compared to the thermal resistance of the surface to air heat flow. Therefore, the thermal resistance across the interface between the pipe and the fins was neglected in all of the calculations.

Thirty-four fins were machined and sand blasted for the experiment. However, the length of the aluminum pipe restricted the number which could be used on runs with wide spacing. Also, the difficulty encountered in sliding several of the fins along the tube resulted in the discarding of some of these fins. For a majority of the runs twenty-seven fins were used.

The weight of the steel fins necessitated the use of a supporting rack for the test section. The test section was mounted so that it was inclined downward at approximately three degrees toward the collection tank. This incline caused the condensate within the tube to run into the collection tank and not back into the steam line.

The saturation tank (see Fig. 7) was part of the permanent laboratory equipment. The purpose of this tank was to change the superheated inlet steam from the university power plant into saturated steam. The tank was equipped with a Bourdon tube pressure gage and thermometer wells. A partial-immersion thermometer was used

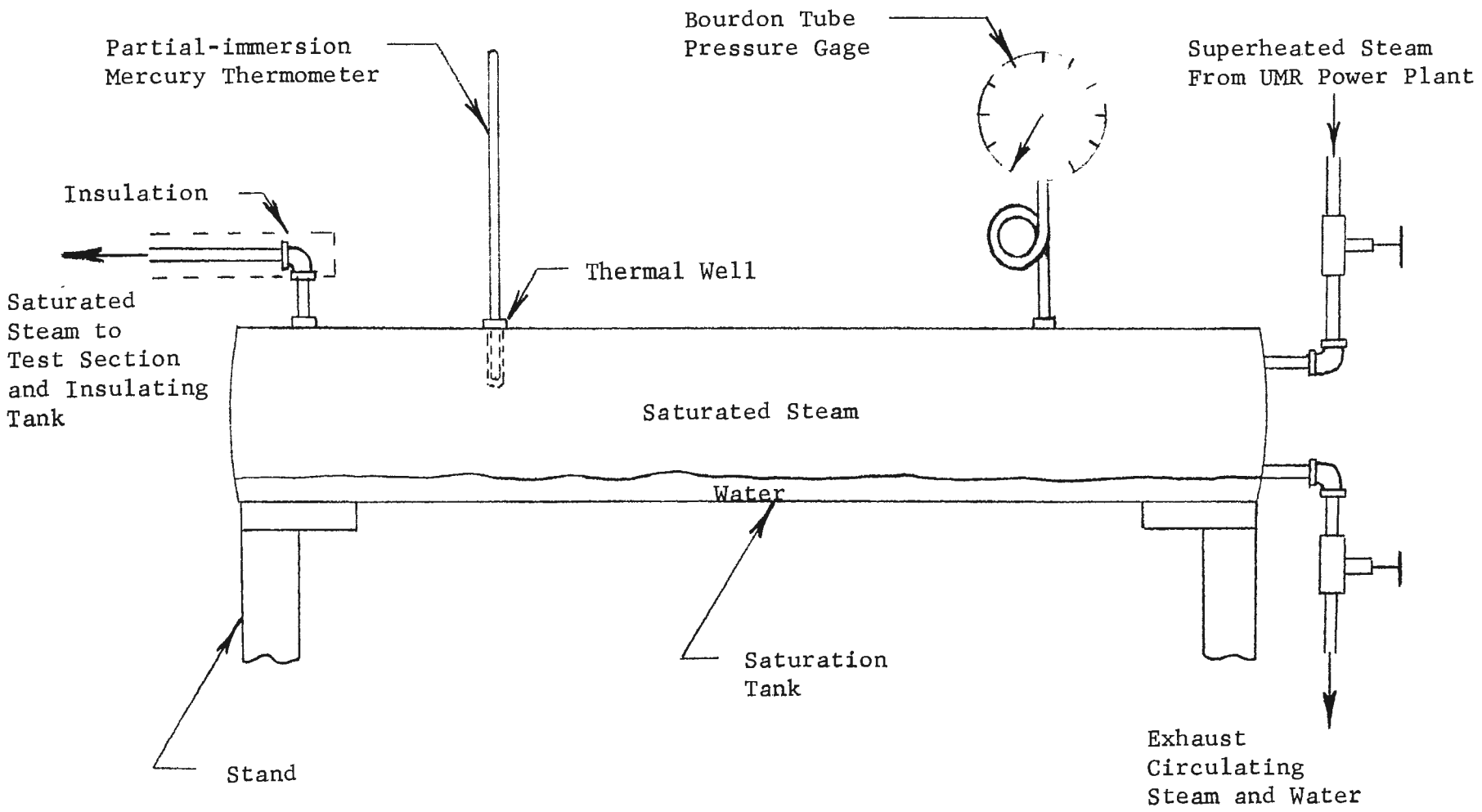

FIG. 7 - SATURATION TANK ASSEMBLY

to check the steam temperature and insure that saturated steam was present in the tank. A three-eighths-inch insulated pipe ran from the top of this tank to a tee from which one line ran to the test section and the other line to the insulating tank enclosing the condensate-collection tank.

The condensate-collection tank was located at one end of the test section and was enclosed in the larger insulating tank. High pressure valves were used to prevent any steam leakage during the tests. All of the pipes were covered with magnesia pipe insulation with the exception of the test section.

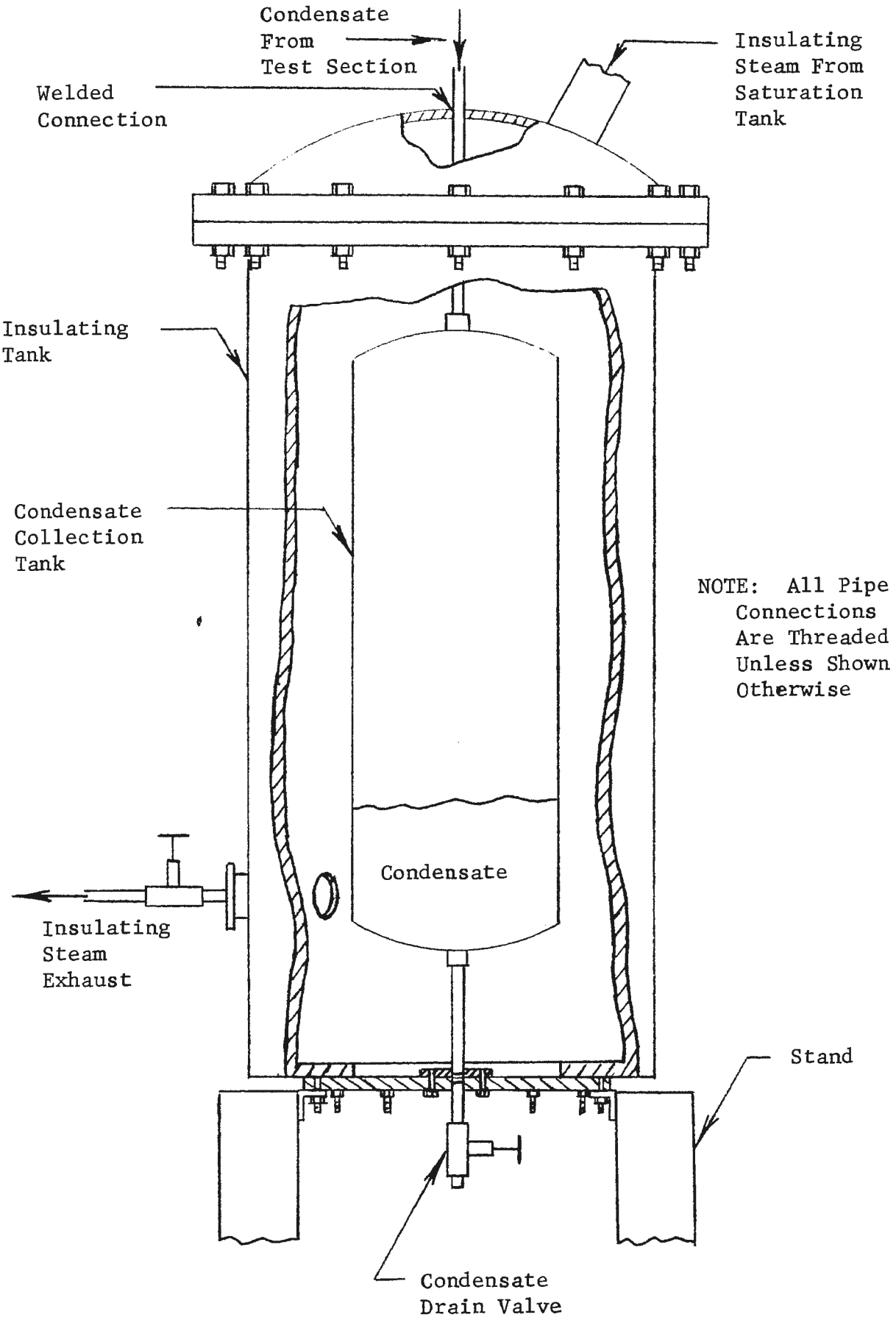

FIG. 8 - COLLECTION TANK ASSEMBLY

IV. EXPERIMENTAL PROCEDURE

Experimental data was taken for fin spacings ranging from zero to one and one-half inches. The first run was made with no spacing between the thirty-four fins. Insulation was placed on all of the steam-supply pipes and the condensate-transfer line. Two, flat, three-quarter-inch-thick plates of magnesia insulation were placed against the end fins.

The exhaust valves on the collection tank, saturation tank, and the insulating tank were all opened before the steam was turned on at the beginning of each test run. The steam valve was then opened slightly and the air was purged from the apparatus. When all of the air was driven out, the valve on the condensate-collection tank was closed completely, while the exhaust valves on the saturation tank and the insulating tank remained slightly open throughout each run. The exhaust valves were left partially open in order to keep the steam circulating and to exhaust the excess condensate in these tanks. Then the apparatus was allowed to sit with the steam at line pressure of 152 psig in order for the test section to reach steady-state conditions. It usually took approximately one hour for the apparatus to reach equilibrium at narrow fin spacing while wider spacings required less time.

A radiation pyrometer was focused onto a smear of black pipe-joint compound placed on the outer edge of the fins in order to determine the fin temperature. This black pipe-joint compound had a measured emissivity of unity, and, consequently, radiated heat as a black body. This made temperature measurements easier to obtain.

When this temperature reached a steady value, it was assumed that the test section was at equilibrium.

After the steady-state condition was reached, the valve on the bottom of the collection tank was opened to clear the tank of condensate collected during the warm-up period for the apparatus. Then this valve was closed and the two-hour test run was begun. During the run, measurements were made of the steam pressure, room temperature, and the fin temperatures on the outer radius at various fins along the test section.

When the run was completed, the shut-off valve between the test section and the condensate-collection tank was closed and the steam was allowed to exhaust from the remainder of the apparatus. The collection tank was then allowed to cool until the temperature of the steam and condensate within the tank cooled and reduced the pressure from 152 psig to a vacuum. It took approximately one hour to cool sufficiently. The vent valve on top of the collection tank was then opened and the condensate was drained from the bottom of the tank. The volume and temperature of the condensate were measured.

After the test section had reached room temperature, the fins were spaced for the next run and the same procedure was followed for each run.

Several runs were made to obtain data for checking calculations, although this data was not used directly in determining the heat transfer per unit length of finned section. Two runs were made with insulation on the test tube and no fins on the section. These runs

were made to determine the volume of condensate resulting from heat losses and from the steam trapped within the collection tank at the end of each run. The volume of condensate which was obtained was 600 ml.

The emissivities of the aluminum tube and the steel fins were determined experimentally using the radiation pyrometer. A smear of black pipe-joint compound was placed on the surface of the saturation tank and the temperature measurement was taken with the radiation pyrometer. The true temperature of the tank was known and so the emissivity of the pipe-joint compound was determined to be approximately 1.0, since the pyrometer read the true temperature for this value of emissivity. Then the compound was placed on the aluminum pipe and the steel fins. The temperatures were measured by using an emissivity setting of 1.0. Then the pyrometer was focused on the bare metal and by knowing the true temperature, the radiation pyrometer gave values for the emissivities. These values were checked at several intervals during the course of the experiment and were observed to remain constant.

VI. REDUCTION OF DATA

The volume and temperature of the condensate collected for each fin spacing was measured in order to calculate the total heat-transfer rate from the section. To obtain the volume of saturated steam which condensed as a result of the heat flow from the test section, it was necessary to substract 600 ml of condensate to account for extraneous losses during the time interval of two hours for each run. This figure also included the condensate from the steam which was trapped inside the collection tank at the end of each run. Next, the remaining volume was divided by the length of the test section in order to obtain the condensate per unit length of finned section. The condensate was converted to pounds mass and then the equivalent heat-transfer rate in BTU/hr-ft was calculated using the heat of vaporization for steam at the test pressure. The values obtained are tabulated in the appendix and are shown on a graph in the results section.

Theoretical calculations were made to reduce this data into a form which would show the heat transfer by radiation and by convection from each portion of the finned section. The total heat-transfer rate consisted of heat transfer from 1) the outside radius of the fins, 2) the aluminum pipe, and 3) the lateral fin surfaces.

The convection heat-transfer coefficient from the outside radius of the fins was calculated, using the formula $\bar{N}u = C(GrPr)^m$, where the properties of the air were evaluated at the experimental temperature observed on the fin at each spacing and C and m are constants. McAdams (13) has listed values for the constants C and m

for various ranges of the Grashof-Prandtl number product. The assumption was made that even for wide spacings the average heat-convection coefficient could be calculated using the theory of a horizontal, circular cylinder. This assumption introduced very little error because the difference in the heat-convection coefficient for a horizontal cylinder and a vertical, flat plate is only approximately seven per cent. In addition, this area was a very small portion of the total fin area.

The radiation heat transfer from the outer fin radius was calculated using the radiation coefficient evaluated at the experimental fin tip temperature for each spacing. The radiation coefficient which was used is shown below:

$$\bar{h}_r = \epsilon\sigma(T^4 - T_a^4)/(T - T_a).$$

An experimentally-determined value of $\epsilon = 0.65$ for the steel was used for these calculations. This value for emissivity was obtained by using the radiation pyrometer.

The radiation and convection heat transfer from the aluminum pipe were calculated at a temperature of 365°F using the same theoretical equations for the radiation and convection coefficients as were used for the outer radius of the fins. An experimentally-determined value of $\epsilon = 0.13$ was used for the emissivity of the aluminum tube.

The geometric shape factor for circular plates was given in the theory section of this report. Since the desired quantity was the radiation heat-transfer rate from the section to the surroundings, the heat-transfer rate was expressed in terms of one minus the shape

factor for radiation between adjacent fins. According to radiation network theory, the heat-transfer rate by radiation from the lateral surfaces of each fin to the surroundings was given by the following formula:

$$q_r = \frac{2A_1\sigma(T_1^4 - T_a^4)}{\frac{1}{\epsilon_{st}} - 1 + \frac{1}{(1 - F_{1-2})}} .$$

The outside surface temperatures of the fins were used for these calculations since most of the radiation heat transfer to the surroundings came from near the outer radius of the fins. This was especially true for narrow fin spacings.

By substracting from the measured total heat-transfer rate the sum of the heat-transfer rates from the ends of the fins, the aluminum tube, and the radiation from between the fins, the heat-transfer rate by convection from the lateral fin surfaces could be evaluated. The convection heat-transfer rate from between the fins has been plotted on a graph in the results section of this report.

VI. DISCUSSION OF RESULTS

Unwanted heat losses occurred during each run primarily from two sources. One source was the heat loss from the valves between the test section and the collection tank and the valve at the bottom of the collection tank. None of these valves were covered with insulation during the runs. The other loss was due to the condensate which was present in the bottom of the insulating tank surrounding the condensate-collection tank and was at a slightly lower temperature than the steam surrounding the collection tank. The lower temperature was due to the heat loss from the bottom and sides of the insulating tank.

The test equipment was allowed to sit approximately one hour in order to reach steady-state conditions before each run was made. Therefore, approximately the same loss rate occurred during each run. In order to determine the magnitude of the total heat-loss rate, a run was made without fins and with insulation covering the aluminum test section. The volume of condensate collected during this run represented both the heat-loss rate and the condensate from the steam entrapped in the collection tank at the end of each run. The volume of condensate from this run was substracted from the total condensate for each run before calculations were made.

The major source of error encountered during the experimental work was due to variations in room temperatures. The room temperature was recorded during each run and has been recorded in the appendix of this report. All theoretical calculations were made for a room temperature of 90°F, which was close to the average value

of experimental room temperatures.

The experimental data has been presented graphically in Fig. 9, Fig. 10, and Fig. 11, and the calculations were tabulated in Appendix E. The curve of heat-transfer rate as a function of fin spacing shows how critical the spacing is to obtain a maximum heat-transfer rate per unit length of the test section. Beginning at zero spacing and proceeding toward wider spacings, it was observed that the overall heat-transfer rate per unit length actually decreased very slightly before starting to increase. This phenomenon was explained by considering the heat transfer from the outer radii of the fins. When there is no spacing, the total outer surface area transferred heat by convection and by radiation. Then as the spacing was introduced, the outer surface area per unit length was decreased because of the air gaps between the fins. This decrease in surface area reduced the heat transfer by convection by an amount proportional to the decrease in surface area.

The heat transfer by radiation from the fin outer surface was also reduced in proportion to the surface area; however, the air gaps emitted radiation as though they were black-body surfaces. Actually, the radiation from between the fins came from the lateral fin surfaces, but at this narrow spacing, the calculations were approximately the same as though the radiation were considered as coming from the air gaps, and this representation was much easier to visualize. Although the radiation heat-transfer rate increased slightly, the convection heat-transfer rate per unit length was reduced more than enough to compensate for the increase from radiation and

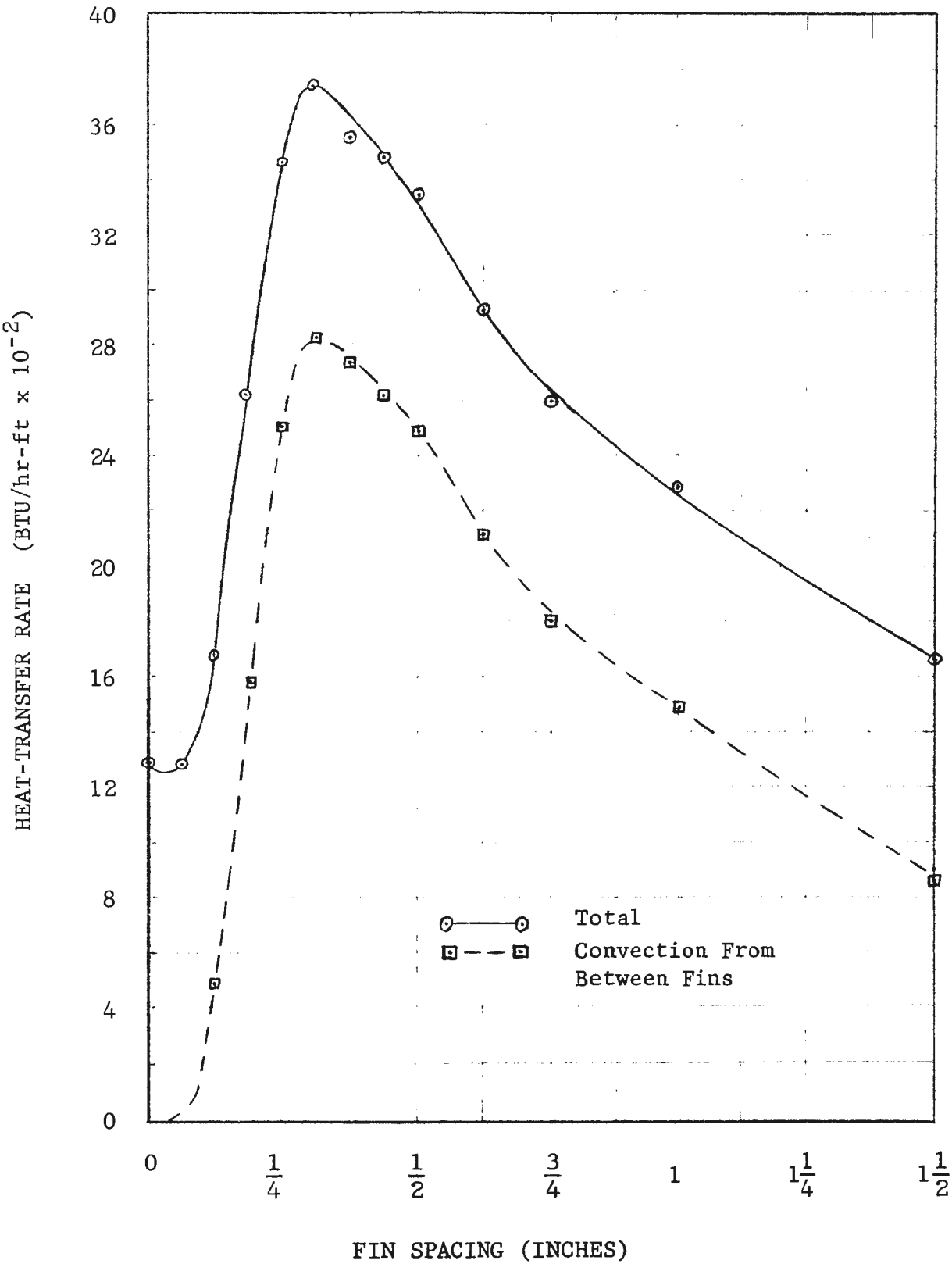

FIG. 9 - HEAT-TRANSFER RATE AS A FUNCTION OF FIN SPACING

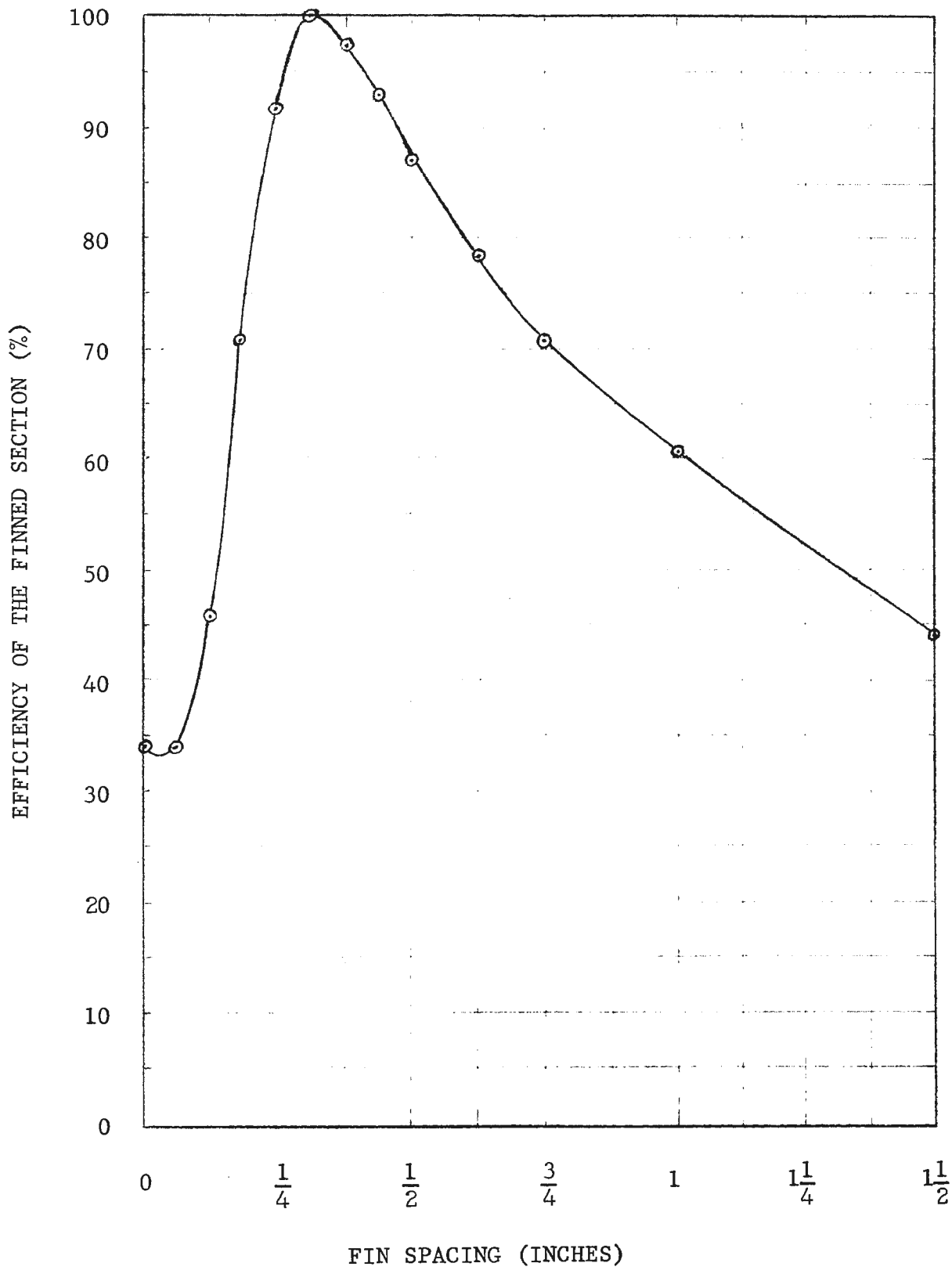

FIG. 10 - EFFICIENCY AS A FUNCTION OF FIN SPACING

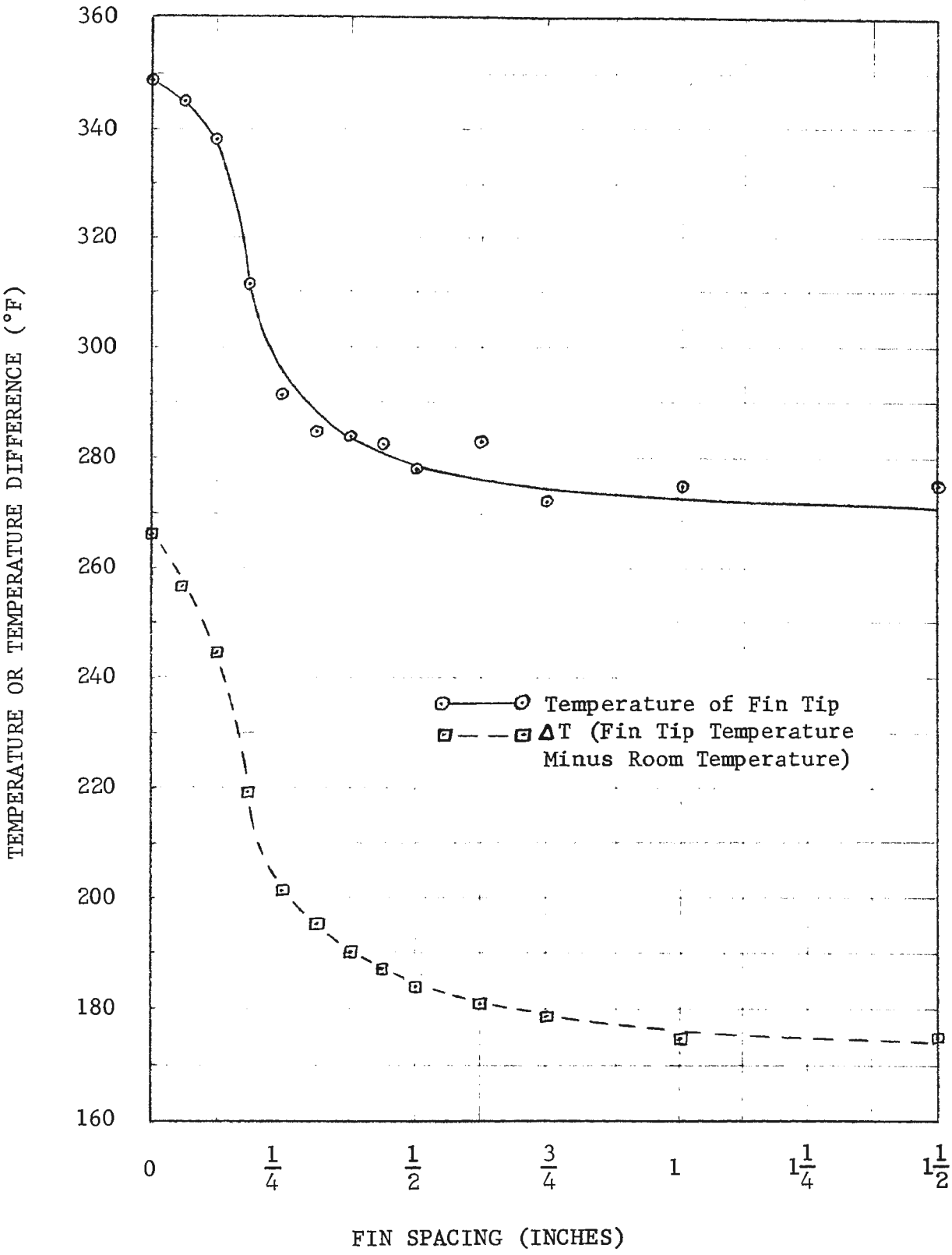

FIG. 11 - FIN TIP TEMPERATURE AS A FUNCTION OF FIN SPACING

consequently, the overall heat-transfer rate per unit length decreased for the very narrow fin spacings.

As the spacing was enlarged over one-sixteenth of an inch, the convection heat-transfer rate from between the fins began to increase rapidly. This great increase in the heat-convection coefficient was a result of the air gap becoming wide enough to allow some of the heated air to rise and carry the heat away.

The theory of heat transfer from a vertical, flat surface to air by free convection depends upon the development of a thermal boundary layer which consists of moving masses of heated air. This heated air rises as a result of the density variation with the surrounding cooler air. For this study, the flow rate was assumed to be laminar across the entire fin surface.

For wide spacings, the thermal boundary layers from adjacent fins did not overlap and the heat-convection coefficient for the lateral fin surfaces was observed to be identical with the theoretical value for a vertical, flat plate. Then, as the fins were placed closer together, the overlapping of boundary layers began to cause a reduction in the convection heat-transfer coefficient on the lateral fin surface. But the increase in surface area due to more fins per unit length actually caused an increase in the overall heat-transfer rate per unit length by convection from the lateral fin surfaces. Finally, at five-sixteenths of an inch, the point was reached at which the maximum heat-transfer rate per unit length was observed. This spacing was designated as the optimum fin spacing. It should be noted that this was not the point of maximum

heat transfer from the test section. The total heat-transfer rate continued to increase with wider spacings because the test section was longer. But the heat transfer per unit length of the test section was a maximum at this optimum spacing.

As the spacing was decreased below the optimum spacing, the convection heat-transfer coefficient from between the lateral fin surfaces was greatly reduced, and the total heat-transfer rate per unit length decreased as a result of this.

The "efficiency of the finned section" was defined in the Introduction of this report to be "the ratio of the actual heat-transfer rate per unit length to the heat-transfer rate at the optimum fin spacing." From the graph of Fig. 10, it could be seen that the efficiency of the finned section was reduced rapidly by spacings either too narrow or too wide, especially if the spacing was too small. Of course, the definitions of fin efficiency or fin effectiveness should still be used to determine the performance of a single fin. But for a finned section, the additional information concerning 'the efficiency of the finned section' would be of interest when the fin itself has already been designed.

In applications, such as aircraft and space vehicles, where the weight of the finned section is of more importance than space, then the efficiency should be figured using the heat-transfer rate per unit weight. Because the steel fins are so heavy, the bare aluminum tube would transfer more heat to the air per unit weight than any fin spacing arrangement.

The experimental results were verified by theoretical calculations for zero spacing and for 'wide' spacing. At zero fin spacing the theoretical radiation and convection coefficients were evaluated at the experimental surface temperature. At 'wide' fin spacing the convection coefficient had to be evaluated at the average surface temperature. The assumption was made that a constant value for the heat-convection coefficient could be used to determine the temperature distribution along the fin profile. This assumption allowed the use of an equation written in terms of Bessel functions to describe the temperature distribution along the circular fin of rectangular profile. The procedure for these operations has been included in the appendix of the report.

The equation was derived by writing an energy balance in a differential ring of a circular fin and expressing this in terms of cylindrical coordinates. When this equation was evaluated and plotted on log-log paper, the temperature distribution could be approximated by a straight line. This made it possible to express the temperature distribution in the form of a power equation, i.e., $T(r) = Cr^m$, where C is the temperature at r = 1.0 and m is the slope of the line on log-log paper. Then, by integrating the product of the temperature and the differential area over the surface of the fin, and then dividing by the fin area, the average temperature on the fin surface was obtained in the form shown below:

$$T_{avg} = \frac{1}{A} \int_{r_i}^{r_o} 2\pi r T(r) dr \ .$$

The average value of the heat-convection coefficient was cal-

culated using the average temperature on the fin surface. By knowing the temperature on the inside radius of the fin, the fin properties, and the fin dimensions, it was possible to obtain theoretical values for the fins' outer radii temperatures and then the heat-transfer rate by convection from the lateral fin surfaces. The calculations in the appendix show how the trial and error method of solution was used for simultaneously solving the Bessel equation for the outside radius temperature and the equation for the heat convection coefficient using the average temperature on the surface. The experimental value for the convection heat-transfer rate from the lateral fin surface at one and one-half inch spacing was 125 BTU/hr-fin while the theoretical calculations gave a value of 129 BTU/hr-fin.

No theoretical formulas were found in any reference books which would enable calculations to be made for transfer rate at spacings where the thermal boundary layers overlapped. However, some suggestions by the author are presented in the recommendations section of this report for a possible method of determining the heat-transfer rate by convection at the optimum fin spacing.

The average temperature on the outside radius of each fin was recorded and has been presented graphically on Fig. 11. The shape of this curve shows that the outside radius temperature decreases in proportion with the increase in convection heat-transfer rate from between the fins. Because this outside temperature is a function of the convection from between the fins, it has been suggested in the recommendations section that the outer radius temperature at the optimum fin spacing may be approximated theoretically.

There was a slight error introduced into the experimental data by placing insulation on the outer surface of the fin at each end of the test section. During each run the temperatures on the outer radii of several fins were measured and very little effect from the insulation was noted at a distance of two or more fins from the end. At very narrow spacings the end fins tended to reach a steady-state temperature of five to ten degrees below the average outer radii temperatures of the other fins. And at large spacings, the insulation tended to keep the end fins warmer than the other fins because the end fins could transfer heat away only on one side.

The thermal resistance between the condensing steam and the inside of the tube is of small magnitude in comparison with the thermal resistance between the outside surface areas and the air. (11) Also, the contact thermal resistance between the tube and fins is of a very small magnitude in comparison with the surface to air resistance. However, the magnitudes of these resistances to heat flow are of no concern as long as heat is conducted past the resistances and the surface temperature on the fin can be measured at steady-state conditions. The only use which was made of the thermal resistance within the steel fins was to determine the temperature distribution along the fin profile.

VII. CONCLUSIONS

The experimental data showed that the optimum fin spacing for convection heat transfer to air at a room temperature of 90°F occurred at five-sixteenths of an inch for the particular test section used in this experiment with an inside radius temperature of 365°F. The optimum fin spacing will be affected by fin height, fin surface temperature, ambient temperature, gravity, and the viscosity, volumetric coefficient of expansion, and the density of the heat-transfer fluid. Therefore, in order to predict an optimum spacing for a finned section it would be necessary to consider all of these factors.

The shape of the curve showing the heat-transfer rate as a function of the fin spacing indicates how critical the optimum spacing is for maximum heat transfer per unit length. If "the efficiency of the finned section" is defined as "the ratio of the actual heat transfer to the heat transfer per unit length at the optimum fin spacing", this efficiency drops off rapidly when the optimum fin spacing is either over or under estimated.

Heat is transferred away from a finned section by radiation and by convection from all exposed surfaces. However, the heat transfer by convection from between the fins is primarily responsible for the heat-transfer rate at surface temperatures in the range of 300°F to 500°F. This indicated that in order to obtain the maximum overall heat-transfer rate, the heat-transfer rate per unit length by convection from between the lateral fin surfaces should be maximized.

Because the temperature distribution at the optimum spacing was not known, the average surface temperature could not be calculated. As a result, the experimental heat-transfer rate at the optimum fin spacing could not be verified theoretically.

VIII. RECOMMENDATIONS

A. Suggested Extension of This Study

The purpose of this investigation, which was to obtain an optimum fin spacing, has been accomplished. However, the optimum fin spacing will probably be different for various set-ups since this optimum spacing depends upon the height of the fin, gravity, ambient air temperature, fin surface temperature, and the properties of the air evaluated at the average surface temperature of the fin. W. Elenbaas (4) has given a theoretical equation for calculating the optimum fin spacing and the average heat-convection coefficient for air from between vertical, flat plates at uniform temperature. Extended surfaces do not have uniform temperatures so this equation cannot be applied directly. It would first be necessary to determine an average temperature over the fin surface and then make the assumption that the entire fin surface were at the average temperature. In order to do this it would be necessary to know the temperature distribution along the fin. Then, for a circular fin of rectangular profile, the average temperature would be given by the equation below.

$$T_{avg} = \frac{1}{A} \int_{r_i}^{r_o} 2\pi r T(r) dr$$

The temperature on the outer radius of a circular fin with 'wide' fin spacings can be calculated by solving the Bessel equation for the temperature distribution in a circular fin of rectangular profile along with the theoretical equation for the heat-convection coefficient for a vertical, flat plate. The heat-convection coefficient would be necessary to solve for the temperature distribu-

tion and the average surface temperature would be necessary to solve for the heat-convection coefficient. Consequently, these equations must be solved by trial and error. The method described was used in this report for theoretically determining the outer radius temperature at 'wide' spacings, and the method has been outlined in Appendix C of this report.

By experimentally determining the optimum fin spacing for several different fin sizes, materials, and temperatures, the fins' outer radii temperatures for the optimum fin spacings could be determined. Then, perhaps from this data a formula could be derived for obtaining the outer radius temperature at the optimum spacing as a function of the inner radius temperature and the outer radius temperature at 'wide' spacings.

If the temperature distribution along the fin profile were known at the optimum fin spacing, the average surface temperature could be evaluated and the optimum spacing and the heat-transfer rate could be calculated. The temperature distribution along fins with no spacing between them will have the form of a log curve.(Fig.12) The Bessel equation which gives the temperature distribution along a fin at 'wide' spacing can be approximated by an equation of the power form. It would seem reasonable that the temperature distribution along the fin profile at the optimum fin spacing would be somewhere between these two extreme conditions.

Experimental data could be taken to determine the heat-transfer rate at the optimum spacing for fins of various materials, sizes, and surface temperatures. From the data it could be determined what

average temperature was necessary in order to use the theoretical equation for convection heat transfer as presented in the theory section of this report. Then, by correlating the data from various runs, the required temperature distribution at the optimum spacing could be determined.

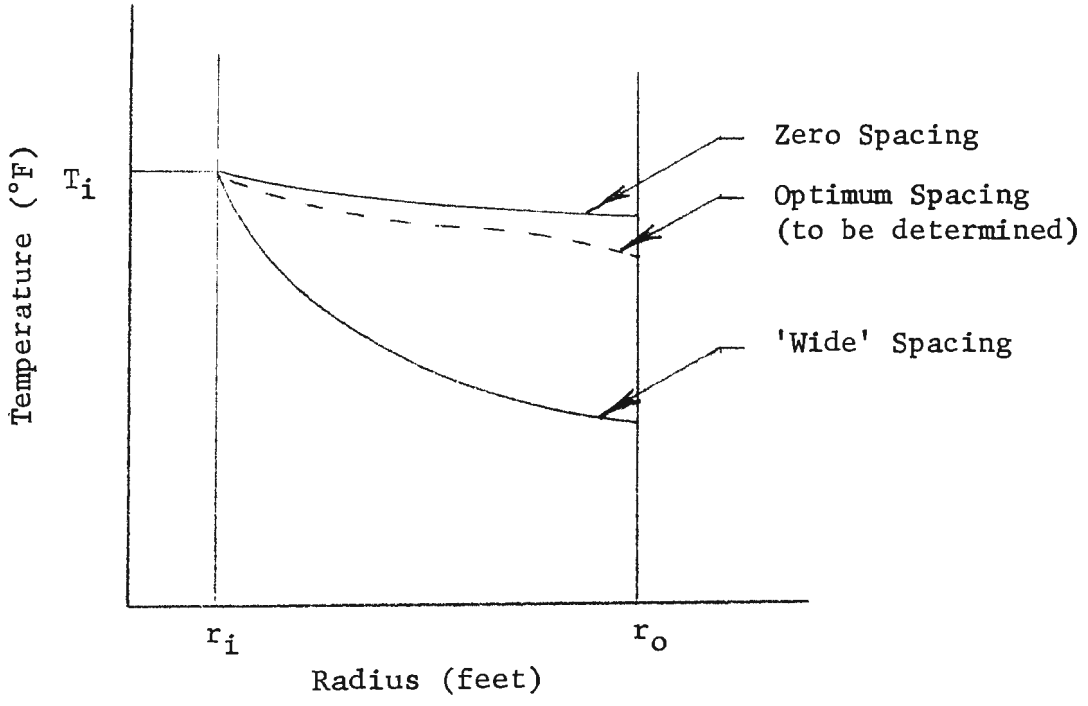

FIG. 12 - PROPOSED TEMPERATURE DISTRIBUTION ALONG FINS AT OPTIMUM FIN SPACING

Therefore, if the outside radius temperature and the temperature distribution could be predicted at the optimum fin spacing, the optimum spacing and the heat-transfer rate at this spacing could be calculated.

B. Improvements in Experimental Operations

The author recommends a change in the test apparatus if the equipment which was used in this investigation is to be used for

further studies. The steam exhaust from the insulating tank should be taken from the bottom, instead of the side, of the tank. This would eliminate the heat-loss rate from the collection tank to the condensate within the insulating tank.

The author also recommends that the test apparatus be placed in a room where the ambient temperature may be held constant throughout the investigation.

BIBLIOGRAPHY

1. Brown, Aubrey I. and Marco, Salvatore M., Introduction to Heat Transfer, third edition, McGraw-Hill Book Company, Inc., New York, 1958.

2. Durham, Franklin P., Thermodynamics, second edition, Prentice-Hall, Inc., New Jersey, 1961.

3. Elenbass, W. "Dissipation of Heat by Free Convection," Parts I and II, Philips Research Report 3, N. V. Philips' Gloeilampenfabrieken, Eindhoben, Netherlands, 1948, pp. 338-360 and 450-465.

4. Elenbaas, W., Physica 9, 1, 1942.

5. Elenbaas, W., Physica 9, 865, 1942.

6. Hamilton, D. C. and Morgan, W. R., National Advisory Committee for Aeronautics, Technical Note 2836, Purdue University, December 1952.

7. Hartog, J. P. Den, Advanced Strength of Materials, McGraw-Hill Book Company, Inc., New York, 1952.

8. Higdon, Archie, Ohlsen, Edward H., and Stiles, William B., Mechanics of Materials, John Wiley and Sons, Inc., New York, 1960.

9. Holman, J. P., Heat Transfer, McGraw-Hill Book Company, New York, 1963.

10. Keenan, Joseph H. and Keyes, Frederick G., Thermodynamic Properties of Steam, thirty-sixth printing of first edition, John Wiley and Sons, Inc., New York, 1964.

11. Kreith, Frank, Principles of Heat Transfer, second edition, International Textbook Company, Pennsylvania, January 1966.

12. Laschober, Robert R. and Sward, Glenn R., ASHRAE Paper 2028, "Correlation of the Heat Output of Unenclosed Single and Multiple-Tier Finned-Tube Units," February 16, 1967.

13. McAdams, W. H., Heat Transmission, third edition, McGraw-Hill Book Company, Inc., New York, 1954.

14. Schneider, P. J., Conduction Heat Transfer, Addison-Wesley Publishing Company, Inc., Massachusetts, 1957.

VITA

The author, Glenn Ellis Miller, was born on August 6, 1944, in West Plains, Missouri. He received his elementary and high school education at Mountain View Public Schools located in Mountain View, Missouri. From September 1962, to June 1966, he attended the University of Missouri at Rolla. Upon graduation with a Bachelor of Science Degree in Mechanical Engineering, the author was commissioned a 2/Lt., USAR. He obtained a delay of active duty with the U.S. Army and received an appointment as a Graduate Teaching Assistant in the Mechanical Engineering Department at the University of Missouri at Rolla for the academic year 1966-67, while he began working toward an M.S. Degree in Mechanical Engineering. On June 3, 1967, the author married Joy Earle Meserve of Independence, Missouri.

APPENDIX A

DERIVATION OF HEAT - CONVECTION COEFFICIENT THEORY (9)

A differential equation describing the motion of the convection heat-transfer boundary layer within the laminar flow region has been obtained by using a momentum analysis along with an energy equation. Both of these equations were derived for an elemental control volume within a laminar portion of the boundary layer.

The momentum equation is derived by writing a balance for the momentum flux in the direction parallel with the vertical surface, referred to hereafter as the x-direction. The momentum flux is the product of the mass flow and the component of velocity in that direction. By equating the sum of the external forces in the x-direction to the change in momentum flux through the control volume and by using the continuity relation $\left(\frac{\partial u}{\partial x} + \frac{\partial v}{\partial y} = 0\right)$, the momentum equation becomes:

$$(1) \qquad \rho \left[u\frac{\partial u}{\partial x} + v\frac{\partial u}{\partial y}\right] = \mu \frac{\partial^2 u}{\partial y^2} - \frac{\partial p}{\partial x} - \rho g .$$

By using $\frac{\partial p}{\partial x} = -\rho_\infty g$ and expressing the density difference in terms of the volumetric coefficient of thermal expansion, β, the equation takes the form:

$$(2) \qquad \rho \left[u \frac{\partial u}{\partial x} + v \frac{\partial u}{\partial y}\right] = g \rho \beta (T - T_a) + \mu \frac{\partial^2 u}{\partial y^2} .$$

The velocity component normal to the surface is neglected and the momentum equation, integrated over the boundary layer thickness (δ), is expressed as:

$$(3) \qquad \frac{d}{dx}\left[\int_0^\delta \rho u^2 dy\right] = -\mu \left.\frac{\partial u}{\partial y}\right]_{y=0} + \int_0^\delta g \beta (T - T_a) dy .$$

The velocity and temperature distributions within the boundary layer are obtained by applying boundary conditions to equation (3). The temp-

erature distribution is given as:

$$(4) \qquad \frac{T-T_a}{T_w-T_a} = \left(1 - \frac{y}{\delta}\right)^2 .$$

The velocity distribution is obtained by assuming the velocity to be a polynomial function of y multiplied by an arbitrary function of x. Denoting this arbitrary function of x as u_x, a fictitious velocity, the velocity distribution is shown as:

$$(5) \qquad \frac{u}{u_x} = \frac{y}{\delta} \left(1 - \frac{y}{\delta}\right)^2 .$$

Inserting these expressions for the velocity and temperature distributions into equation (3) and carrying out the mathematical operations gives:

$$(6) \qquad \frac{1}{105} \frac{d}{dx} (u_x^2 \delta) = \frac{1}{3} g \beta (T_w - T_a) \delta - \nu \left[\frac{u_x}{\delta}\right] .$$

The energy equation is obtained by considering the elemental control volume within the laminar boundary layer with the following assumptions.

1. Incompressible, steady flow
2. Constant viscosity, thermal conductivity, and specific heat
3. Negligible heat conduction in the direction of flow

Writing an energy balance gives the energy equation for the laminar portion of the boundary layer:

$$(7) \qquad u \frac{\partial T}{\partial x} + v \frac{\partial T}{\partial y} = \alpha_t \frac{\partial^2 T}{\partial y^2} + \frac{\mu}{\rho C_p} \left[\frac{\partial y}{\partial y}\right]^2 .$$

The term containing the viscosity, μ, may be neglected when considering free convection because the velocity is so low. This low velocity causes the viscous work term to be negligible in comparison with the conduction term. So for free convection the energy equation becomes:

$$(8) \qquad u \frac{\partial T}{\partial x} + v \frac{\partial T}{\partial y} = \alpha_t \frac{\partial^2 T}{\partial y^2} .$$

Integrating this with respect to y gives:

$$(9) \qquad \frac{d}{dx}\left[\int_0^{\delta} u(T - T_a)\,dy\right] = \alpha_t \frac{dT}{dy}\Big]_{y=0} .$$

Now substituting the velocity and temperature distributions into equation (9) gives:

$$(10) \qquad \frac{1}{30}(T_w - T_a)\,\frac{d}{dx}(u_x\,\delta) = 2\,\delta_t\left[\frac{T_w - T_a}{\delta}\right] .$$

The differential equations (6) and (10) are solved simultaneously by assuming that both u_x and δ have a variation with x of the following form: $u_x = c_1 x^m$ and $\delta = c_2 x^n$ These constants are evaluated as:

$$(11) \qquad C_1 = 5.17\nu\left[\frac{20}{21} + \frac{\nu}{\alpha_t}\right]^{-\frac{1}{2}}\left[\frac{g\,\beta\,(T_w - T_a)}{\nu^2}\right]^{\frac{1}{2}}, \text{ and}$$

$$(12) \qquad C_2 = 3.93\left[\frac{20}{21} + \frac{\nu}{\alpha_t}\right]^{\frac{1}{4}}\left[\frac{g\,\beta\,T_w - T_a)}{\nu^2}\right]^{-\frac{1}{4}}\left[\frac{\nu}{\alpha_t}\right]^{-\frac{1}{2}} .$$

From these calculations, the boundary layer may be expressed as a function of the distance from the edge of the surface in terms of the Prandtl and Grashof numbers as:

$$(13) \qquad \frac{\delta}{x} = 3.93\ Pr^{-\frac{1}{2}}\ (0.952 + Pr)^{\frac{1}{4}}\ Gr_x^{-\frac{1}{4}} .$$

From Fourier's Law and the temperature distribution in equation (4), the value of the heat convection coefficient may be evaluated.

$$(14) \qquad q_w = -kA\frac{dT}{dy} = hA\,(T_w - T_a) .$$

$$(15) \qquad h = -\frac{k\frac{dT}{dy}}{T_w - T_a} = -\frac{k}{(T_w - T_a)}\,(T_w - T_a)\,(-\frac{2}{\delta}) = \frac{2k}{\delta} .$$

Since Nusselt's number is defined as $\frac{hx}{k} = \frac{2x}{\delta}$, then the heat-convection coefficient may be expressed in terms of the following dimensionless equation:

$$(16) \qquad Nu_x = 0.508\ Pr^{\frac{1}{4}}\ (0.952 + Pr)^{-\frac{1}{4}}\ Gr_x^{\frac{1}{4}} .$$

For much experimental work, the value for the average heat-convection coefficient has been expressed as:

$$(17) \qquad \frac{\bar{h}L}{k} = \bar{Nu} = C\,(Gr\ Pr)^m ,$$

where the properties are evaluated at the mean film temperature, defined as:

$$(18) \qquad T_f = \frac{T_a + T_w}{2} .$$

The values for C and m have been determined experimentally by McAdams (13) for various ranges of the Grashof - Prandtl number product.

APPENDIX B

SAMPLE CALCULATION FOR HEAT TRANSFER BY CONVECTION FROM THE END OF THE FINS

These calculations were for zero spacing between the fins and a surface temperature of 350°F with an ambient temperature of 90°F. The properties of air were evaluated at the mean film temperature, T_f.

$$T_f = \frac{T_w + T_a}{2} = 220°F$$

$$\rho = p/RT = 0.0565 \text{ lb}_m/\text{ft}^3$$

$$C_p = 0.241 \text{ BTU/lb}_m - °F$$

$$\mu = 0.053 \text{ lb}_m/\text{hr} - \text{ft}$$

$$k = 0.0178 \text{ BTU/hr} - \text{ft} - °F$$

$$\beta = 1.48 \times 10^{-3} \ °F^{-1}$$

$$Pr = \frac{C_p \mu}{k} = 0.718$$

$$Gr_d = \frac{g \beta (T_w - T_a) \rho^2 d^3}{\mu^2} = 5.35 \times 10^7$$

$$PrGr_d = 0.384 \times 10^8$$

$$Nu = C(Gr_d \ Pr)^m$$

McAdams (13) has evaluated the constants C and m for $10^4 < PrGr_d < 10^9$ as:

$$C = 0.53 \quad \text{and} \quad m = 0.25 ,$$

$$Nu_d = 41.8 ,$$

$$h_c = \frac{k}{d} Nu_d = 1.15 \text{ BTU/hr} - \text{ft}^2 - °F .$$

The convection coefficients for the various fin spacings required different values because of the change in surface temperature of the fins.

Holman (9) gives the following simplified equation for air at atmospheric pressure when 10^4 PrGr 10^9 and the flow of air is laminar:

$$h_c = 0.27 \left[\frac{\Delta T}{d}\right]^{\frac{1}{4}}.$$

APPENDIX C

CALCULATION FOR CONVECTION HEAT-TRANSFER RATE FROM LATERAL FIN SURFACES AT 'WIDE' FIN SPACING

The temperature distribution along a single fin is given by the following Bessel equation: (14)

$$\frac{T}{T_o} = \left[\frac{I_o(Nr)\ K_1(Nr_{2c}) + I_1(Nr_{2c})\ K_o\ (Nr)}{I_o(Nr_2)K_1(Nr_{2c}) + I_1(Nr_{2c})\ K_o\ (Nr_i)}\right] \quad \text{, where}$$

$T_o = t_w - t_a = 275°F,$

$r_i = 0.0544$ ft,

$r_{2c} = 0.333$ ft,

$k = 27.0$ BTU/hr-ft-°F,

$\delta = 0.0104$ ft,

$N = \sqrt{h/k\delta}$, and

h is to be determined.

The temperature at the end of the fin may be evaluated by setting $r = r_2 = 0.323$ ft ;

$$T_2 = 275\left[\frac{I_o\ (.610\ \sqrt{h})\ \ K_1\ (.629\ \sqrt{h}) + I_1\ (.629\ \sqrt{h})\ \ K_o\ (.610\ \sqrt{h})}{I_o\ (.1025\ \sqrt{h})\ K_1\ (.629\sqrt{h}) + I_1\ (.629\ \sqrt{h})\ \ K_o\ (.1025\ \sqrt{h})}\right] .$$

The average heat convection coefficient may be expressed in terms of the average surface temperature as:

$$\bar{h}_c = 0.29\left[\frac{T_{avg}}{L}\right]^{\frac{1}{4}} = 0.3235\ (T_{avg})^{\frac{1}{4}}.$$

The average surface temperature was next expressed in terms of the end temperature. If the heat convection coefficient is assumed to be constant over the fin surface, then the expression for the temperature distribution is a straight line on log-log paper and may be expressed

in a power form:

$$T(r) = C_1 r^m ,$$

where C_1 = T at r = 1.0 , and

m = slope = $0.562 (\ln T_2 - 5.61)$.

C_1 was also evaluated in terms of T_2 :

$$C_1 = T_2 e^{-1.058m} .$$

$$T_{avg} = \frac{1}{A} \int_{r_1}^{r_2} 2\pi r t(r) dr = \frac{2\pi C_1}{A(m+2)} \left[r_2^{m+2} - r_1^{m+2} \right] .$$

Since T_2 was the only unknown, the value of T_2 was solved for by trial and error methods:

Assume $T_2 = 163°F$,

$m = -0.2835$,

$C_1 = 222$,

$T_{avg} = 173$,

$\bar{h}_c = 1.171$,

$\bar{h}_r = \epsilon\sigma (t_{avg}^4 - t_a^4) / T_{avg} = 1.17$,

$\bar{h}_T = 2.341$ BTU/hr-ft^2-°F,

$$T_2 = 275 \left[\frac{I_o (.940) K_1 (.970) + I_1 (.970) K_o (.940)}{I_o (.158) K_1 (.970) + I_1 (.970) K_o (.158)} \right] = 163°F .$$

The heat-transfer rate by convection from the lateral surfaces of one fin at 'wide' spacing was calculated as:

$$q_c = 2\bar{h}_c A T_{avg} = 129 \text{ BTU/hr-fin} .$$

APPENDIX D

EXPERIMENTAL RESULTS

FIN SPACING (INCHES)	0	1/16	1/8	3/16	1/4	5/16	3/8	7/16	1/2	5/8	3/4	1	1 1/2
LENGTH OF SECTION (INCHES)	8.5	10.75	10.0	11.625	13.24	14.875	16.5	18.125	19.75	23.0	33.25	32.75	31.75
NUMBER OF FINS	34	34	27	27	27	27	27	27	27	27	34	27	19
ROOM TEMPERATURE (°F)	83	88	94	93	93	88	98	92	93	98	97	90	97
FIN TIP TEMPERATURE (°F)	349	345	338	312	291	285	284	282	278	283	272	275	272
TIME OF RUN (HOURS)	2	2	2	2	2	2	2	2	2	2	1 1/2	2	2
VOLUME OF CONDENSATE (MILLILITERS)	1568	1821	2117	3330	4686	5569	5854	6217	6544	6628	6261	7265	5300
TOTAL HEAT-TRANSFER RATE (BUT/HR)	900	1140	1410	2540	3800	4620	4890	5230	5510	5600	7210	6200	4360
HEAT-TRANSFER RATE (BUT/HR-FIN)	26.5	33.6	52.3	94.1	141.0	171.0	181.0	194.0	204.0	207.5	212.0	229.0	230.0
HEAT-TRANSFER RATE (BTU/HR-FT)	1270	1270	1690	2620	3440	3730	3550	3470	3350	2920	2600	2280	1650

APPENDIX E

THEORETICAL RESULTS

FIN SPACING (INCHES)	0	1/16	1/8	3/16	1/4	5/16	3/8	7/16	1/2	5/8	3/4	1	1 1/2
TEMPERATURE DIFFERENCE (FROM GRAPH) (°F)	266	257	244	219	202	195	190	187	184	181	178	175	175
SHAPE FACTOR, F_{1-2}	0	.9845	.9692	.9542	.9395	.9249	.9106	.8965	.8826	.8557	.8295	.7795	.6890
RADIATION FROM BETWEEN FINS (BUT/HR-FIN)	0	5.78	10.6	13.3	15.5	18.4	21.0	23.6	26.3	31.4	36.4	45.9	64.5
FLOW RATE FROM END OF FIN (BTU/HR-FIN)	26.6	26.3	24.4	20.9	18.6	17.8	17.1	16.8	16.4	15.9	15.7	15.2	15.2
FLOW RATE FROM TUBE (BUT/HR-FIN)	0	1.08	2.16	3.23	4.30	5.40	6.46	7.55	8.63	10.8	12.9	17.3	25.9
CONVECTION FROM BETWEEN FINS (BTU/HR-FIN)	0	0	15.1	56.7	102.6	129.4	136.4	146.0	152.7	149.4	147.0	150.0	130.0
CONVECTION FROM BETWEEN FINS (BTU/HR-FT)	0	0	490	1590	2510	2820	2740	2610	2500	2110	1800	1490	850
EFFICIENCY OF THE FINNED SECTION (%)	34	34	46	71	92	100	97	93	87	78	71	61	44